CHEMISTRY
A EUROPEAN JOURNAL

DOI: 10.1002/chem.201201399

Retro-Diels–Alder Approach to the Synthesis of π-Expanded Azuliporphyrins and Their Porphyrinoid Aromaticity

Tetsuo Okujima,*[a] Tasuku Kikkawa,[a] Haruyuki Nakano,[b] Hiroshi Kubota,[a] Nobumasa Fukugami,[a] Noboru Ono,[a] Hiroko Yamada,[c] and Hidemitsu Uno[a]

Abstract: Bicyclo[2.2.2]octadiene (BCOD) fused azuliporphyrins were synthesized by 3+1 porphyrin synthesis of azulitripyrranes with diformylpyrroles. Subsequent retro-Diels–Alder reaction of the BCOD-fused azuliporphyrins afforded azulibenzo-, azulidibenzo-, and azulitribenzoporphyrins **1**–**5**. NMR and UV/Vis spectra, as well as nucleus-independent chemical shift (NICS) calculations revealed that **1**–**5** and their diprotonated dications exhibit relatively low porphyrinoid aromaticity, which was dependent on the position and number of fused benzene rings present.

Keywords: ab initio calculations · cations · conjugation · electronic structure · porphyrinoids

Introduction

Core-modified heteroanalogues of porphyrins have been studied extensively because of their unique and interesting properties, for example, their altered core sizes and resulting metal-ion-binding properties.[1] Azuliporphyrin, one of the carbaporphyrins, was reported by Lash and co-workers for the first time in 1997.[2a] Since then, various azuliporphyrin derivatives, such as *meso*-free,[2] *meso*-aryl,[3a] core-modified,[3b,4] ring-expanded,[3f] and contracted[5a] azuliporphyrins, as well as their metal complexes,[3c,d] *adj*-diazuli,[3e] *opp*-diazuliporphyrins,[5b,c] and tetraazuliporphyrin tetracation,[5d] have been reported. As expected from its resonance structures, the azulene subunit interrupts the conjugative pathway within the macrocycle (Figure 1, structure **I**), whereas the azuliporphyrin also contributed to the zwitterionic resonance structure **II** as a macrocyclic 18 π-electron system. The UV/Vis absorption spectrum of azuliporphyrin in CH_2Cl_2 showed moderate bands between 350 and 480 nm, whereas the ^1H NMR spectrum in $CDCl_3$ shows a weak macrocyclic ring current. In diprotonated azuliporphyrin, delocalization of positive charge generates [18]annulene porphyrinoid aromaticity (Figure 1, structures **IV** and **V**), which was supported by NMR and UV/Vis absorption data. It was therefore concluded that azuliporphyrin had borderline porphyrinoid aromaticity.[2a]

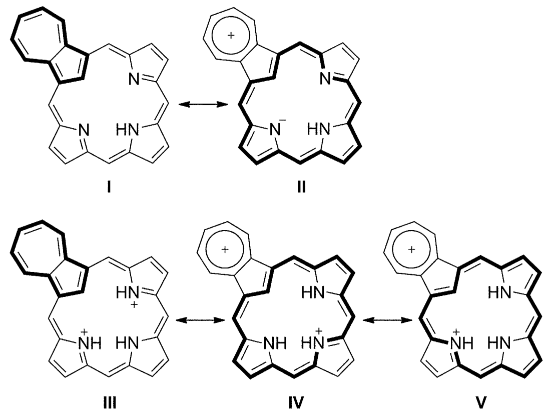

Figure 1. Resonance structures of free base (**I** and **II**) and diprotonated (**III**, **IV**, and **V**) azuliporphyrins.

We have reported a synthesis of azulitribenzoporphyrin by 3+1 porphyrin synthesis by using bicyclo[2.2.2]octadiene (BCOD) fused tripyrrane and azulene-1,3-dicarbaldehyde,[6] and subsequent retro-Diels–Alder conversion of the BCOD moieties into the benzene subunits.[7] However, its aromaticity could not be examined due to its low solubility. The aromaticity of azulibenzoporphyrins is expected to be controlled by the position and number of fused benzene rings, which are localized as a six-π-electron system or included in the macrocyclic π system, accounting for our interest in the aromaticity of such π-expanded azuliporphyrins. In this paper, we report the synthesis of a series of azulibenzoporphyrins **1**–**5** (Figure 2) by the retro-Diels–Alder reaction of

[a] Prof. Dr. T. Okujima, T. Kikkawa, H. Kubota, N. Fukugami, Prof. Dr. N. Ono, Prof. Dr. H. Uno
Graduate School of Science and Engineering
Ehime University
Matsuyama 790-8577 (Japan)
Fax: (+81) 89-927-9615
okujima.tetsuo.mu@ ehime-u.ac.jp

[b] Prof. Dr. H. Nakano
Graduate School of Sciences
Kyushu University
Fukuoka 812-8581 (Japan)

[c] Prof. Dr. H. Yamada
Graduate School of Materials Science
Nara Institute of Science and Technology
Ikoma 630-0192 (Japan)

Supporting information for this article is available on the WWW under http://dx.doi.org/10.1002/chem.201201399.

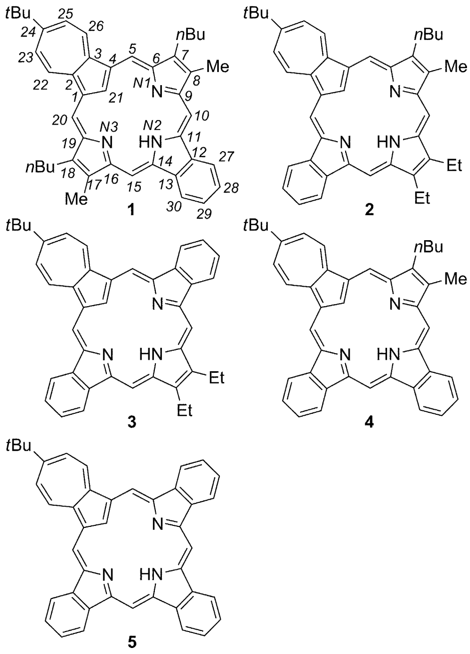

Figure 2. Azulibenzoporphyrins **1**–**5**.

the corresponding BCOD-fused precursors. Their structures, aromaticity, and optical properties were elucidated by NMR, UV/Vis, and X-ray crystallographic analyses, and by theoretical calculations.

Results and Discussion

Azuliporphyrins have been readily prepared by condensing tripyrrane with azulene-1,3-dicarbaldehyde,[2a,7] or azulitripyrrane with pyrrole-1,3-dicarbaldehyde under 3+1 conditions.[2b] We adopted the latter method as our synthetic approach because azulitripyrranes are relatively stable compared with tripyrranes. This approach required only three types of azulitripyrranes to afford all desired azulibenzoporphyrins, whereas five tripyrranes would have been necessary for the former method. The preparation of azulitripyrranes **10**–**12** is shown in Scheme 1. Condensation of 6-*tert*-butylazulene (**6**)[8] with two equivalents of **7** in CH_2Cl_2 with montmorillonite K-10 clay[9] gave azulitripyrrane **10** in 78% yield, after column chromatography on alumina and recrystallization from $CHCl_3$/hexane. BCOD-fused azulitripyrrane **11** was obtained similarly by the reaction of **6** with two equivalents of **8**,[7,10] in 79% yield. Unsymmetrical azulitripyrrane **12** was the stating material used to prepare **2** and **4**. Montmorillonite-catalyzed stepwise condensation of **6** with **8** and **7** afforded **12** in two steps.

The synthesis of BCOD-fused azuliporphyrins **15**–**19** based on the 3+1 methodology is shown in Scheme 2. Tripyrrane **10** was treated with trifluoroacetic acid (TFA) to remove the ester groups, and the resulting mixture was diluted with CH_2Cl_2 and treated with dialdehyde **13**.[11] After oxidation with $FeCl_3$, work-up of the reaction mixture and purification by column chromatography and recrystallization, *opp*-BCOD-fused azuliporphyrin **15** was furnished in 32% yield. *Adj*-di- and tri-BCOD-fused azuliporphyrins **16** and **17** were obtained by analogous reactions of **11** with **14** and **13** in 46 and 35% yields, respectively. Tripyrrane **12** reacted with **14** and **13** under similar conditions to afford *adj*-mono- and *adj*,*opp*-di-BCOD-fused azuliporphyrins **18** and **19**, respectively. The thermal conversion processes of BCOD-fused azuliporphyrins were investigated by using thermogravimetric analysis (results shown in the Supporting Information, Figure S1). The weight loss from **15** and **17** started at 140 and 130°C and finished at 190 and 180°C, respectively. The amounts lost from **15** and **17** were 4.5 and 12.5%, respectively, corresponding to the removal of ethylene molecules, closely matching the calculated values of 4.4 and 12.8%, respectively. When **15**–**19** were heated in the solid state at 200°C in a glass tube under reduced pressure, the corresponding azulibenzoporphyrins **1**–**5** were formed in nearly quantitative yields without purification. These azuliporphyrins were characterized by physical and spectral methods, including X-ray crystallographic analysis for **1**–**3**.

The UV/Vis absorption spectra of BCOD-fused azuliporphyrins **15**–**19** in CH_2Cl_2 are shown in the Supporting Information, Figure S2. Four moderate bands were observed at 300–500 nm, whereas broad, weak bands were observed at 550–800 nm. In 1% TFA/CH_2Cl_2, BCOD-fused azuliporphyrins showed strong Soret-like bands at 360 and 460 nm,

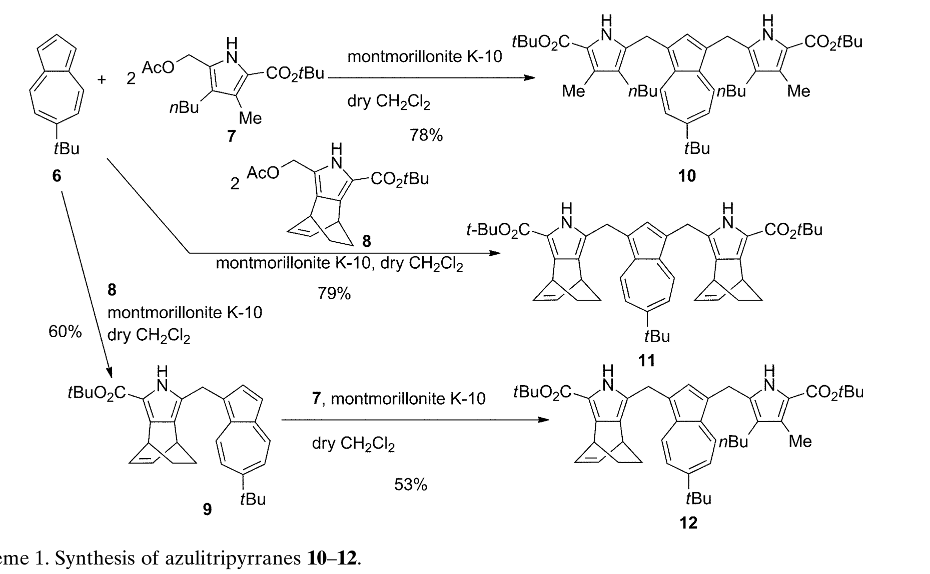

Scheme 1. Synthesis of azulitripyrranes **10**–**12**.

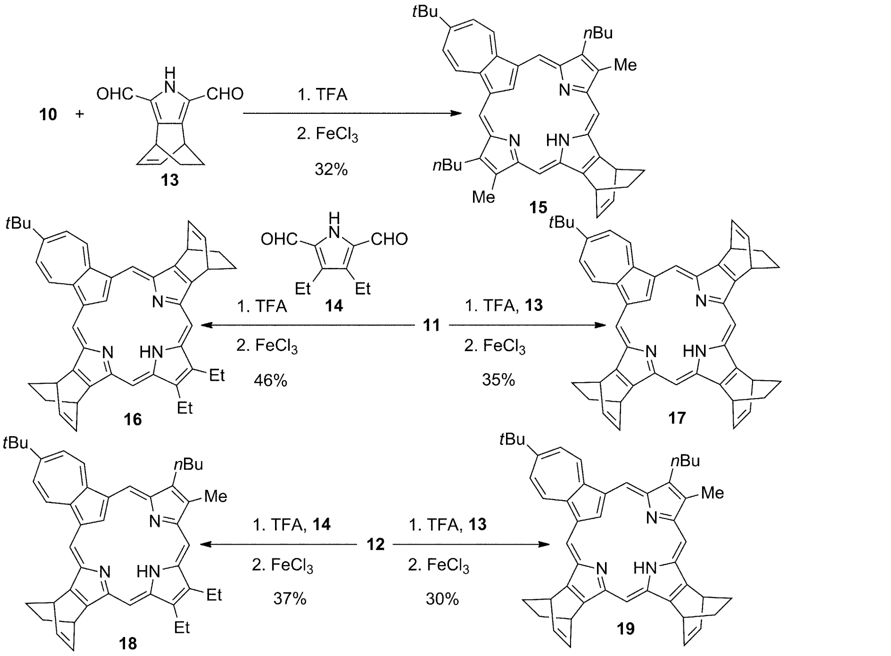

Scheme 2. Synthesis of BCOD-fused azuliporphyrins **15**–**19**.

maxima of azulidibenzoporphyrins **3** (731 nm) and **4** (699 nm) were at wavelengths similar to those found for azulitribenzoporphyrin **5** (736 nm) and azulibenzoporphyrin **2** (694 nm), respectively. The absorption spectra of free-base mono-, di-, and tribenzoporhyrins were comparable.[12] In azulidibenzoporphyrin, diprotonated **4** did not contribute the 26-π-electron structure **4(2H)d^{2+}**, but rather the 22-π-electron structures **4(2H)b^{2+}** and/or **4(2H)c^{2+}**, whereas diprotonated **3** contributed the 26-π-electron structure **3(2H)b^{2+}**. In azulitribenzoporphyrin, the resonance contribution of diprotonated **5** was represented by a combination of 26-π-electron structures, as shown in Figure 6.

and weak Q-like bands at 600–800 nm (see the Supporting Information, Figure S3). The general appearance of the spectrum did not change with the concentration of TFA in CH_2Cl_2. The differences in the absorption spectra of **15**–**19** in CH_2Cl_2 from those in 1% TFA/CH_2Cl_2 were similar to those observed for β-alkylazuliporphyrins.[2a] No effect was observed arising from differences in the position or number of BCOD rings. Diprotonated **15**–**19** contributed to the 18-π-electron structures **IV** and **V** in Figure 1, showing Soret- and Q-like bands. On the other hand, azulibenzoporphyrins **1**–**5** showed different spectra to those obtained from BCOD-fused or β-alkylazuliporphyrins. Broad, split absorptions appeared at 300–500 nm in CH_2Cl_2, as shown in the Supporting Information, Figure S4. The broad, longest-wavelength absorptions at 550–800 nm were slightly redshifted as the number of fused benzene rings increased. The absorptions changed dramatically in 1% TFA/CH_2Cl_2, depending on the position and number of fused benzene rings. The absorption spectra of azulibenzoporphyrins **1** and **2** are shown in Figure 3. Diprotonated **1** and **2** showed Soret-like bands at 365 and 468 nm, and 376 and 463 nm, respectively, which indicated that **1** and **2** possessed porphyrinoid aromaticity similar to **15**–**19** due to the contribution of the [18]annulene structure in 1% TFA/CH_2Cl_2. The longest-wavelength absorption maxima of **1** and **2** were observed at 671 and 694 nm, respectively. Thus, diprotonated **2** contributed not only the 18-π-electron structure **2(2H)c^{2+}**, but also the 22-π-electron structures **2(2H)b^{2+}** and/or **2(2H)d^{2+}**, whereas diprotonated **1** mainly contributed the 18-π-electron structure **1(2H)b^{2+}**, as shown in Figure 4. Azulidibenzo- and azulitribenzoporphyrins **3**–**5** showed moderate broad bands instead of intense Soret-like bands at 350–550 nm in 1% TFA/CH_2Cl_2 (Figure 5). The longest-wavelength absorption

To estimate the electron distribution of azulibenzoporphyrins **1**, **2**, and their diprotonated dications, we performed B3LYP/6-31G(d) density functional theory calculations of HOMO and LUMO orbitals

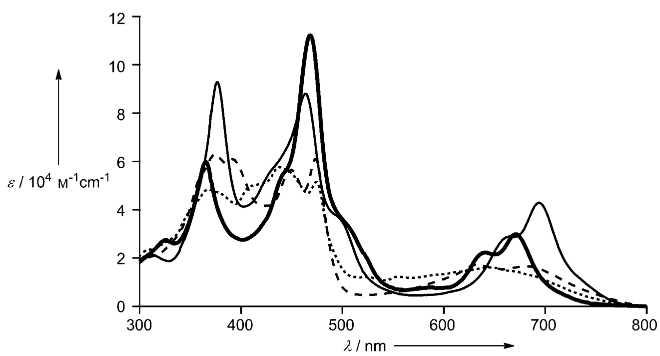

Figure 3. UV/Vis absorption spectra of **1** (dotted) and **2** (dashed) in CH_2Cl_2, and **1** (bold) and **2** (plain) in 1% TFA/CH_2Cl_2.

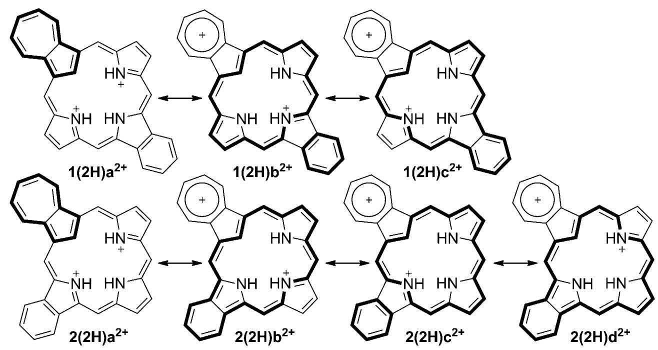

Figure 4. Resonance structures of diprotonated azulibenzoporphyrins **1** (top) and **2** (bottom).

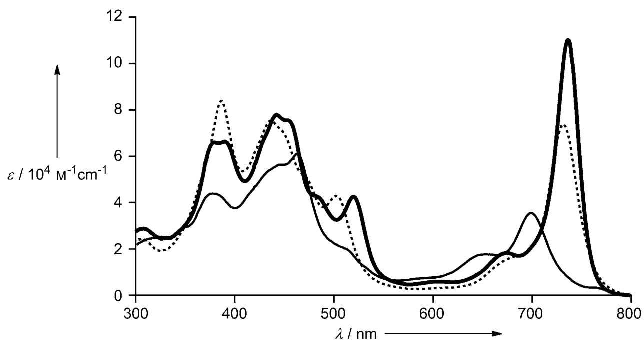

Figure 5. UV/Vis absorption spectra of **3** (dotted), **4** (solid), and **5** (bold) in 1% TFA/CH_2Cl_2.

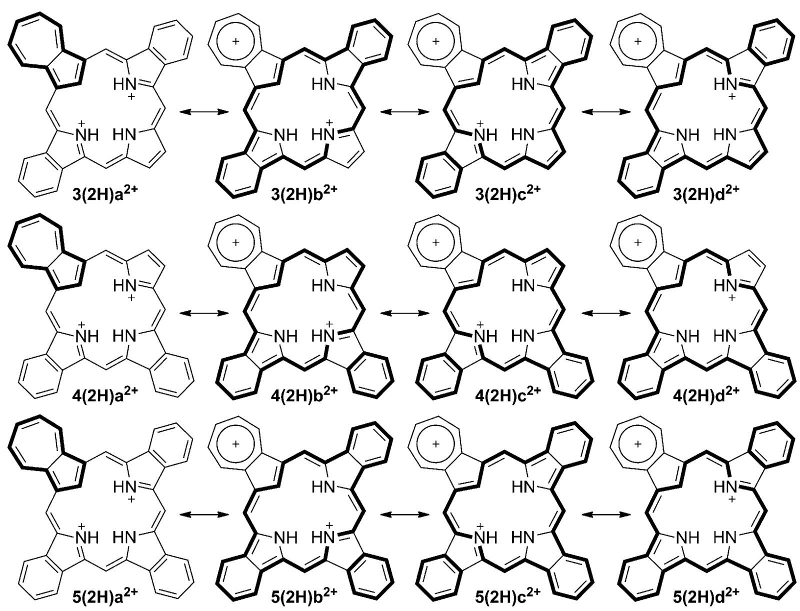

Figure 6. Resonance structures of diprotonated azulidibenzoporphyrins **3** (top) and **4** (middle), and azulitribenzoporphyrin **5** (bottom).

(see the Supporting Information, Table S3). The electron distribution of **1** was quite similar to that of **2** for the four orbitals, LUMO+1, LUMO, HOMO, and HOMO−1 (see the Supporting Information, Figure S5 and S7). The HOMO–LUMO energy gap of **2** (ΔE=2.00 eV) was narrower than that of **1** (ΔE=2.21 eV). The TD-DFT results of **1** and **2** predicted absorptions at 560 and 576 nm, respectively, which corresponded to a broad band at 600–750 nm. Both bands mainly consist of two single-electron transitions, HOMO−1 to LUMO (48% for **1** and 51% for **2**) and HOMO to LUMO+2 (33% for **1** and 27% for **2**). On the other hand, the electron distribution of **1(2H)**$^{2+}$ was different to that of **2(2H)**$^{2+}$, as shown in the Supporting Information, Figure S6 and S8. The HOMO–LUMO energy gap of **2(2H)**$^{2+}$ (ΔE=2.21 eV) was narrower than that of **1(2H)**$^{2+}$ (ΔE=2.42 eV). The TD-DFT results of **1(2H)**$^{2+}$ and **2(2H)**$^{2+}$ predicted absorptions at 587 and 622 nm, respectively. These bands mainly consist of two single-electron transitions, HOMO to LUMO (62%) and HOMO−1 to LUMO+1 (32%) for **1(2H)**$^{2+}$ and HOMO−1 to LUMO (43%) and HOMO to LUMO (27%) for **2(2H)**$^{2+}$. LUMO+1 and LUMO+2 in **1(2H)**$^{2+}$ showed a different distribution to those in **2(2H)**$^{2+}$. The electron distributions in **1(2H)**$^{2+}$ and **2(2H)**$^{2+}$ depended on the fused benzene rings in contrast to those in **1** and **2**, which resulted in a remarkable shift in their absorption spectra.

The ^{1}H NMR spectra of **1**–**3** showed a weak macrocyclic-ring current compared with β-alkylazuliporphyrin (Figure 7). The signals for *meso*-H (H-5, 10, 15, and 20) and internal CH (H-21) appeared at δ=8.73 (H-5, 20), 8.22 (H-10, 15), and 3.74 ppm (H-21) for **1**; δ=9.31 (H-5), 8.99 (H-20), 8.43 (H-10), 8.16 (H-15), and 2.81 ppm (H-21) for **2**; and δ=9.09 (H-5, 20), 8.35 (H-10, 15), and 2.50 ppm for **3**, whereas the signals of β-alkylazuliporohyrin appeared at δ=9.55 and 8.64 ppm for *meso*-H and δ=1.59 ppm for internal CH.[2a] The signals for *meso*-H were shifted upfield or downfield owing, not only to the macrocyclic ring current, but also to the ring currents of neighboring benzene and azulene moieties. The difference in chemical shift between internal CH and peripheral CH increased slightly from **1** to **3**. For azulibenzoporphyrins **1** and **2**, internal CH for **2** was shifted upfield compared with that for **1** due to the strong ring current, which indicated that **2** possessed slightly greater aromaticity than **1**. On the other hand, diprotonated **1**–**3** showed stronger diatropicity than the corresponding free bases. The ^{1}H NMR spectra of diprotonated **1**–**3** are shown in Figure 8. Diprotonated **1**–**3** showed downfield-shifted signals for *meso*-H and upfield-shifted broad-singlet signals for internal CH compared with those of the free bases. Their signals appeared at δ=10.24 (H-5, 20), 9.74 (H-10, 15), and −2.18 ppm (H-21) for **1**; δ=10.57 (H-5), 10.41 (H-20), 9.87 (H-10), 9.63 (H-15), and −2.87 ppm (H-21) for **2**; and δ=10.66 (H-5, 20), 9.96 (H-10, 15), and −2.31 ppm (H-21) for **3**. These results suggested that the dications of azulibenzoporphyrins possessed greater aromaticity than their respective free bases. For diprotonated azulibenzoporphyrins, the difference in chemical shift between internal CH and peripheral CH indicated that fused benzene at the adjacent position for azulene resulted in greater aromaticity compared with fused benzene at the opposite position. The macrocyclic-ring currents of **1**–**3** were weaker for the free bases and stronger for the dications relative to β-alkylazuliporphyrin.[2] The ^{1}H NMR spectra of azu-

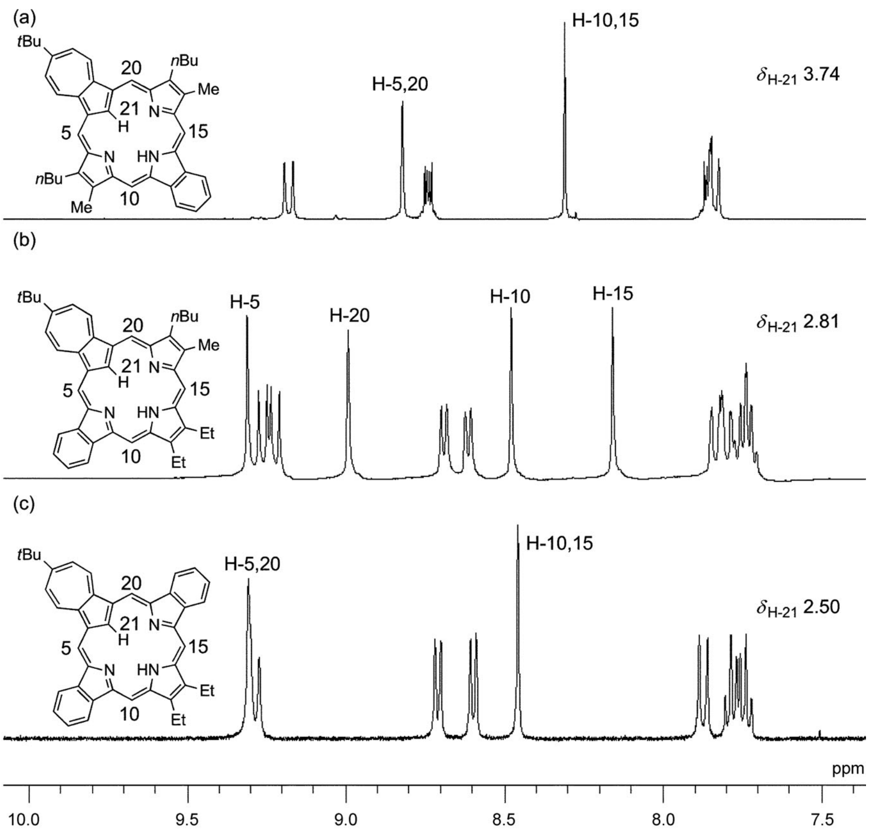

Figure 7. ^{1}H NMR spectra of a) **1**, b) **2**, and c) **3** in $CDCl_3$.

lidibenzo- and azulitribenzoporphyrins **4** and **5**, unfortunately, could not be measured in 5% TFA/$CDCl_3$ due to their low solubility.

Single crystals suitable for X-ray structure determination were obtained after recrystallization from hexane/$CHCl_3$. The molecular structures of **1**, **2**, and **3** are shown in Figure 9 and Figure 10, and the crystallographic data[13–16] are summarized in the Supporting Information, Table S1. *Opp*-azulibenzoporphyrin **1** crystallized in a monoclinic cell, space group $P2_1/c$, $Z=4$, whereas *adj*-azulibenzoporphyrin **2** crystallized in a triclinic cell, space group $P\bar{1}$, $Z=4$. Molecules of **2** exhibited two independent forms with an interplane distance of approximately 3.62 Å. Azulidibenzoporphyrin **3** crystallized with a molecule of $CHCl_3$ in a triclinic cell, space group $P\bar{1}$, $Z=2$. The C−C and C−N bond lengths, except for those of peripheral alkyl groups in azulibenzoporphyrin **1**, are summarized in Table 1. The C−C bond lengths of the benzene rings were all almost the same, 1.377(4)–1.403(3) Å, which indicated that the fused benzene ring was localized as a six-π-electron system. When a pyrrole was replaced with an azulene, resulting in bond-alternation, the average differences in length of adjacent bonds was approximately 0.05 Å for the C−N bonds, approximately 0.1 Å for the C−C bonds of pyrrolic rings, and approximately 0.05 Å for the *meso*-bridging moieties. In the azulene ring, the bonds between C1 (C4) and C2 (C3) were longer than the other peripheral bonds, approximately 1.43–1.44 Å (cf. azulene itself, ca. 1.40 Å).[17] These bond lengths for the benzene moiety, bond-alternation, and the longer bonds between C1 (C4) and C2 (C3) were similar to those observed for **2** and **3** (see the Supporting Information, Table S2).

Nucleus-independent chemical shifts (NICS)[18] have been used as a good indicator of the aromaticity of porphyrins[19] and their core-modified analogues, such as N-confused,[20] hydroxybenzi-,[21] dioxadiazuli-,[5c] and phosphaporphyrins.[22] NICS values were calculated for azuliporphyrin **20**, azulibenzoporphyrins **1**–**5**, and diprotonated **1**–**5** and **20** at the centers of the five- and seven-membered rings of the azulene, the three pyrroles, the fused benzene rings, and the porphyrin macrocycle as a whole. The results are depicted in Figure 11. Two systems, the azuliporphyrins and their diprotonated dications, showed significantly different NICS signatures. For dication **20(2H)**$^{2+}$, the central NICS value of −10.59 ppm was similar to that of dioxadiazuliporphyrin dication.[5c] On the other hand, the NICS value for **20** was smaller (in absolute value) than that of its diprotonated dication. Thus, neutral azuliporphyrins exhibited low porphyrinoid aromaticity due to a diminished contribution of the 18-π-electron system (structure **II** in Figure 1) compared with diprotonated azuliporphyrins. The NICS values at the five-membered ring of azulene, as well as *adj*- and *opp*-pyrroles to azulene for **20(2H)**$^{2+}$ were −4.08, −13.83, and −11.54 ppm, respectively. These results indicated that the

Table 1. C−C and C−N bond lengths in azulibenzoporphyrin **1**.[a]

Bond	Length [Å]	Bond	Length [Å]	Bond	Length [Å]
C1−C2	1.431(3)	C10−C11	1.365(3)	C20−C1	1.417(3)
C1−C21	1.414(3)	C11−N2	1.380(3)	C2−C22	1.386(3)
C2−C3	1.460(3)	C11−C12	1.459(3)	C22−C23	1.387(3)
C3−C4	1.439(3)	C12−C13	1.403(3)	C23−C24	1.403(4)
C4−C21	1.402(3)	C13−C14	1.444(3)	C24−C25	1.390(3)
C4−C5	1.412(3)	C14−C15	1.378(3)	C25−C26	1.379(3)
C5−C6	1.366(3)	C15−C16	1.411(3)	C26−C3	1.384(3)
C6−N1	1.393(3)	C16−N3	1.343(3)	C12−C27	1.397(3)
C6−C7	1.463(3)	C16−C17	1.462(3)	C27−C28	1.377(4)
C7−C8	1.372(3)	C17−C18	1.357(3)	C28−C29	1.398(4)
C8−C9	1.458(3)	C18−C19	1.473(3)	C29−C30	1.380(3)
C9−N1	1.338(3)	C19−N3	1.386(3)	C30−C13	1.395(3)
C9−C10	1.420(3)	C19−C20	1.371(3)		

[a] Number labels for carbon and nitrogen atoms are shown in Figure 2.

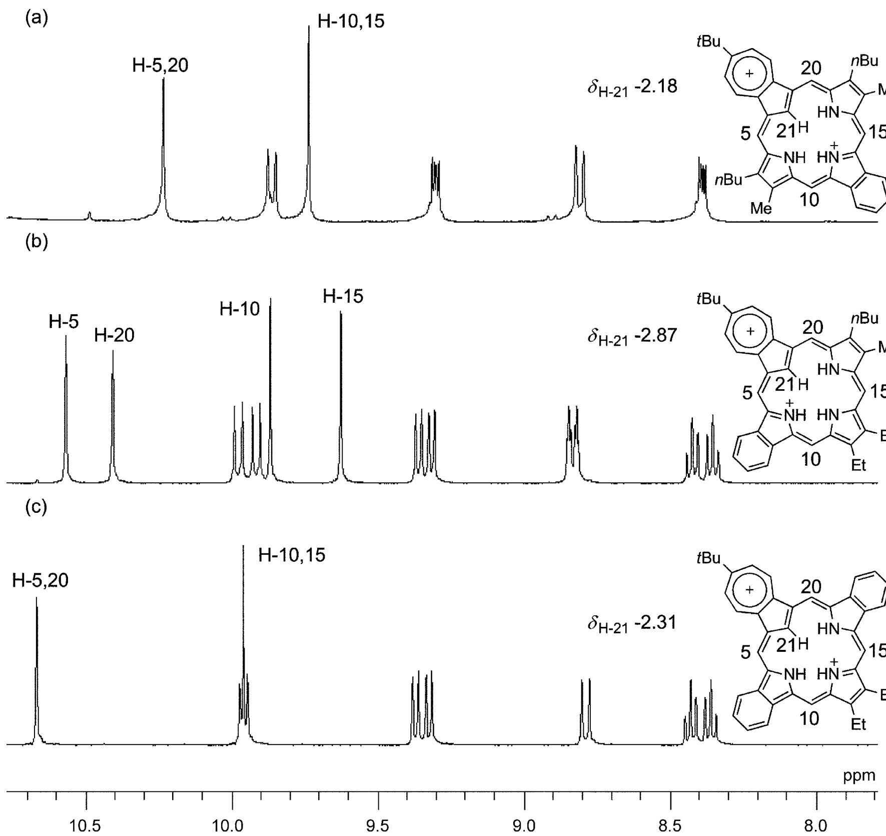

Figure 8. ^{1}H NMR spectra of a) **1**, b) **2**, and c) **3** in 5 % TFA/CDCl$_3$.

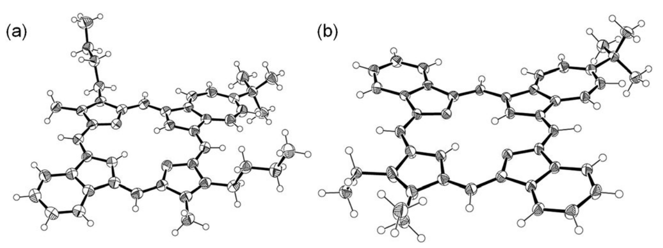

Figure 9. ORTEP drawings of a) **1** and b) **3**. Disordered atoms (less popular: one of the ethyl groups) and a solvent (CHCl$_3$) in **3** are omitted for clarity. Probablility levels are shown at 50 %.

resonance contribution was mainly a combination of structures **IV** and **V**, with a slightly lower contribution of **V**, to show porphyrinoid aromaticity (Figure 1). Increasing the number of fused benzene rings resulted in low porphyrinoid aromaticity. The local six-π-electron benzene aromaticity was preserved in the isoindole moiety with a NICS value of approximately −10 ppm, whereas the fused pyrroles showed lower aromaticity compared with other pyrroles in **1**–**5** and in their dications. For **1(2H)$^{2+}$**, the NICS values at *adj*- and *opp*-pyrroles to azulene were −11.46 and −4.54 ppm, respectively, indicating that **1(2H)$^{2+}$** mainly contributed the structure **1(2H)b^{2+}** (Figure 4). For *adj*-azulibenzoporphyrin **2(2H)$^{2+}$**, the NICS values at *adj*-, *adj*-benzo-, and *opp*-pyrroles to azulene were −14.56, −6.53, and −10.61 ppm, respectively, indicating that **2-(2H)$^{2+}$** was mainly represented by the combination of the resonance structures **2(2H)b^{2+}** and **2(2H)c^{2+}**, although the contribution of **2(2H)b^{2+}** was slightly weaker than that of **2(2H)c^{2+}** (Figure 4). These results are consistent with the longest-wavelength absorptions in the UV/Vis absorption spectra. The porphyrinoid aromaticity depended, not only on the number of fused benzene rings, but also on their positions. For monobenzo-derivatives **1** and **2**, the NICS values of **2** and **2-(2H)$^{2+}$** at the center of the porphyrin macrocycle were larger (in absolute value) than those of **1** and **1(2H)$^{2+}$**, respectively. Similar results were obtained for dibenzo-derivatives. Among the azulibenzoporphyrins, diprotonated *adj*-dibenzo-derivative **3(2H)$^{2+}$** showed the highest aromaticity, with a NICS value of −9.79 ppm at the center of the porphyrin macrocycle. For tribenzo-derivative **5-(2H)$^{2+}$**, the NICS values at the five-membered ring of the azulene, as well as *adj*- and *opp*-pyrroles to azulene were −10.04, −7.31, and −3.80 ppm, respectively, indicating that **5(2H)$^{2+}$** was mainly represented by the combination of resonance structures **5(2H)a^{2+}** and **5(2H)b^{2+}**. Because the contribution of **5(2H)a^{2+}** was more important in the tribenzo-derivative than the monobenzo- and dibenzo-derivatives, **5-(2H)$^{2+}$** possessed lower aromaticity.

Conclusion

We have successfully synthesized a series of azulibenzoporphyrins **1**–**5** based on the retro-Diels–Alder approach from BCOD-fused precursors and unveiled their structures, aromaticity, and optical properties. BCOD-fused azuliporphyrins **15**–**19** were prepared by 3+1 porphyrin synthesis of appropriate azulitripyrranes with diformylpyrroles. These were subsequently converted into the benzo-derivatives **1**–**5** by heating, in nearly quantitative yields. UV/Vis absorption spectra and NICS calculations revealed that the relatively low porphyrinoid aromaticity of **1**–**5** stemmed from the small contribution of the 18-π-electron system due to interruption of the π circuit at the azulene moieties. In contrast, porphyrinoid aromaticity was observed for their diprotonated dications, which were represented by the porphyrinlike π circuit shown in Figure 1. However, their aromaticity was

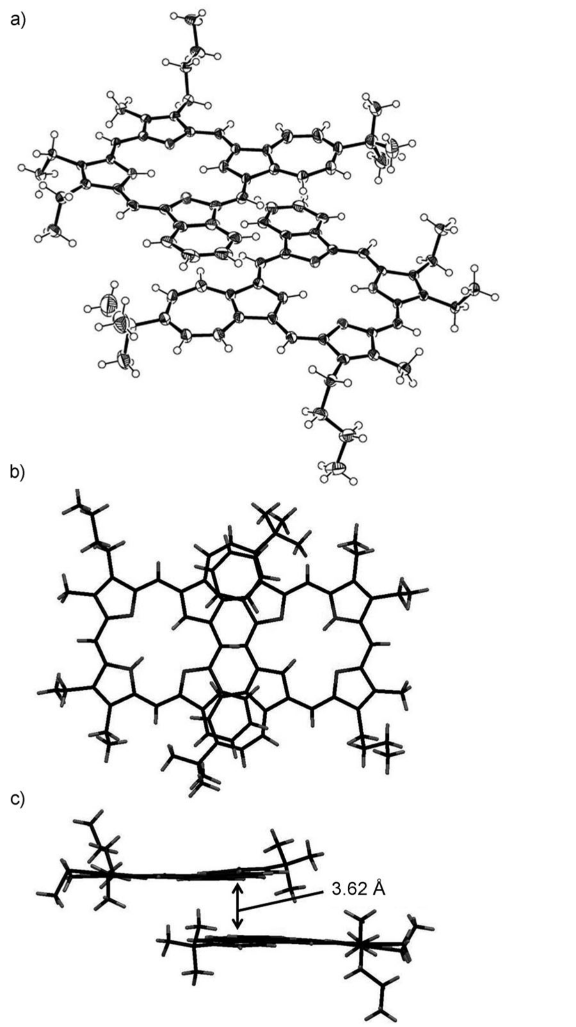

Figure 10. a) ORTEP drawing, b) top, and c) side views of two independent molecules of **2**. Disordered atoms (less popular: one of the butyl groups) are omitted for clarity. Probablility levels are shown at 50 %.

lower than that of azuliporphyrin without fused benzene rings, **20**, and depended on the position and number of fused benzene rings. Benzene subunits were localized in the isoindole moiety. Thus, increasing the number of fused benzene rings resulted in low porphyrinoid aromaticity.

Experimental Section

General: Melting points were determined with a Yanaco micro melting point apparatus MP500D and are uncorrected. DI-EI and FAB mass spectra were measured with a JEOL JMS-700 spectrometer. MALDI-TOF mass spectra were measured with an Applied Biosystems Voyager-DE Pro instrument. TG analysis was performed with an SII Exstar 600 TG/DTA 6200 instrument. IR spectra were measured with a Horiba FT-720 infrared spectrophotometer, and UV/Vis spectra were measured with a JASCO V-570 spectrophotometer. ^{1}H NMR spectra (^{13}C NMR spectra) were recorded with a JEOL AL-400 operating at 400 MHz (100 MHz). Elemental analyses were performed at the Integrated Center for Sciences, Ehime University. NICS values were calculated by using Gaussian 03 (HF/6–31+G(d)//B3LYP/6–31G(d)).

Azulitripyrrane 10: Montmorillonite K-10 clay (7.9 g) was added to a solution of **6** (1.48 g, 8.02 mmol) and **7** (6.19 g, 18.0 mmol) in anhydrous CH_2Cl_2 (220 mL). The resulting mixture was stirred at RT for 20 h under an Ar atmosphere. After the insoluble material was removed by filtration, the filtrate was poured into sat. aqueous $NaHCO_3$. The organic layer was washed successively with water and brine, dried over Na_2SO_4, and concentrated under reduced pressure. The residue was purified by column chromatography on alumina with 20% EtOAc/hexane, followed by recrystallization from $CHCl_3$/hexane to give **10** (4.69 g, 78%). Blue crystals; m.p. 99.0–101.0 °C; ^{1}H NMR (400 MHz, $CDCl_3$): δ=8.13 (brs, 2H; NH), 8.11 (d, J=11.0 Hz, 2H; H-4,8), 7.41 (s, 1H; H-2), 7.24 (d, J=11.0 Hz, 2H; H-5,7), 4.27 (s, 4H; CH_2), 2.46 (t, J=7.1 Hz, 4H; 5′-nBu^1), 2.25 (s, 6H; 4′-Me), 1.47 (s, 18H; 3′-CO_2tBu), 1.43 (s, 9H; 6-tBu), 1.33–1.45 (m, 8H; 5′-nBu^{2,3}), 0.92 ppm (t, J=7.1 Hz, 6H; 5′-nBu^4); ^{13}C NMR (100 MHz, $CDCl_3$): δ=161.75 (C6), 161.24 (3′-CO_2tBu), 137.41 (C2), 135.47 (C3a,8a), 132.44 (C4,8), 131.97 (C1′), 125.94 (C5′), 123.82 (C1,3), 121.55 (C4′), 120.21 (C5,7), 118.22 (C3′), 79.85 (3′-CO_2tBu), 38.52 (6-tBu), 33.31 (5′-nBu^2), 31.83 (6-tBu), 28.51 (3′-CO_2tBu), 24.13 (CH_2), 23.95 (5′-nBu^1), 22.72 (5′-nBu^3), 14.09 (5′-nBu^4), 10.76 ppm (4′-Me); UV/Vis (CH_2Cl_2): λ_{max} [log (ε/M^{-1}cm^{-1})]=241 (4.46), 286 (4.83), 299 (4.86), 340 (3.75), 354 (3.80), 373 (3.35), 595 nm (2.57); MS (70 eV): m/z (%): 683 (16) [M]$^+$, 583 (35), 483 (31), 152 (100); elemental analysis calcd (%) for $C_{44}H_{62}N_2O_4\cdot 1/2H_2O$: C 76.37, H 9.18, N 4.05, found: C 76.59, H 9.09, N 4.18.

Azulitripyrrane 11: Montmorillonite K-10 clay (7.9 g) was added to a solution of **6** (1.46 g, 7.92 mmol) and **8** (5.46 g, 17.2 mmol) in anhydrous CH_2Cl_2 (215 mL). The resulting mixture was stirred at RT for 20 h under an Ar atmosphere. After the insoluble material was removed by filtration, the filtrate was poured into sat. aqueous $NaHCO_3$. The organic layer was washed successively with water and brine, dried over Na_2SO_4, and concentrated under reduced pressure. The residue was purified by column chromatography on alumina with 20% EtOAc/hexane, followed by recrystallization from $CHCl_3$/hexane to give **11** (4.37 g, 79%). Blue crystals; m.p. 154.5–155.9 °C; ^{1}H NMR (400 MHz, $CDCl_3$): δ=8.13 (d, J=10.3 Hz, 2H; H-4,8), 7.86 (brs, 2H; NH), 7.37 (s, 1H; H-2), 7.23 (d, J=10.3 Hz, 2H; H-5,7), 6.46 (m, 4H; H-5′,6′), 4.30 (s, 4H; CH_2), 4.27 (m, 2H; H-4′), 3.67 (m, 2H; H-7′), 1.50 (s, 18H; 3′-CO_2tBu), 1.43 (s, 9H; 6-tBu), 1.34–1.59 ppm (m, 8H; H-8′,9′); ^{13}C NMR (100 MHz, $CDCl_3$): δ=161.69, 161.03, 137.19, 137.16, 136.06, 135.32, 135.23, 132.44, 127.59, 125.90, 124.28, 120.05, 113.51, 79.82, 38.55, 33.90, 32.53, 31.88, 28.58, 27.04, 27.02, 26.41, 24.27 ppm; UV/Vis (CH_2Cl_2): λ_{max} [log (ε/M^{-1}cm^{-1})]=245 (4.50), 290 sh (4.80), 299 (4.83), 343 sh (3.73), 355 (3.79), 370 sh (3.45), 597 (2.57), 655 nm sh (2.48); MS (70 eV): m/z (%): 699 (50) [M]$^+$, 499 (32), 313 (48), 184 (100); elemental analysis calcd (%) for $C_{46}H_{54}N_2O_4\cdot 1/3CHCl_3$: C 75.33, H 7.41, N 3.79; found: C 75.10, H 7.48, N 3.80.

1-(Azulen-1-ylmethyl)isoindole 9: Montmorillonite K-10 clay (3.3 g) was added to a solution of **6** (640 mg, 3.48 mmol) in anhydrous CH_2Cl_2 (60 mL). After stirring at RT for 10 min, a solution of **8** (1.1160 g, 3.5024 mmol) in anhydrous CH_2Cl_2 (45 mL) was added dropwise to the mixture. The resulting mixture was stirred at RT for 12 h under an Ar atmosphere. After the insoluble material was removed by filtration, the filtrate was poured into sat. aqueous $NaHCO_3$. The organic layer was washed successively with water and brine, dried over Na_2SO_4, and concentrated under reduced pressure. The residue was purified by column chromatography on silica gel with CH_2Cl_2, followed by recrystallization from $CHCl_3$/hexane to give **9** (924 mg, 60%). Blue crystals; m.p. 154.5–155.9 °C; ^{1}H NMR (400 MHz, $CDCl_3$): δ=8.22 (d, J=10.5 Hz, 1H; H-4), 8.18 (d, 10.7 Hz, 1H; H-8), 7.83 (brs, 1H; NH), 7.61 (d, J=3.7 Hz, 1H; H-2), 7.32–7.26 (m, 2H; H-5,7), 7.23 (d, J=3.7 Hz, 1H; H-3), 6.53–6.43 (m, 2H; H-5′,6′), 4.35 (s, 2H; CH_2), 4.27 (m, 1H; H-4′), 3.71 (m, 1H; H-7′), 1.54–1.37 (m, 4H; H-8′,9′), 1.50 (s, 9H; 3′-CO_2tBu), 1.44 ppm (s, 9H; 6-tBu); ^{13}C NMR (100 MHz, $CDCl_3$): δ=161.27, 160.94, 139.41, 136.52, 135.99, 135.70, 135.27, 134.57, 132.29, 127.42, 125.98, 120.60, 120.16, 116.15, 113.40, 79.73, 38.49, 33.83, 32.44, 31.86, 31.55, 28.49, 27.01, 26.34, 24.42, 22.66, 14.10 ppm; UV/Vis (CH_2Cl_2): λ_{max} [log (ε/M^{-1}cm^{-1})]=239 (4.36), 285 (4.46), 295 (4.44), 336 (3.67), 349 (3.76), 364 (3.21), 580 nm (2.51); MS (70 eV): m/z (%): 442 (8) [M]$^+$, 342 (26), 184 (100); elemental

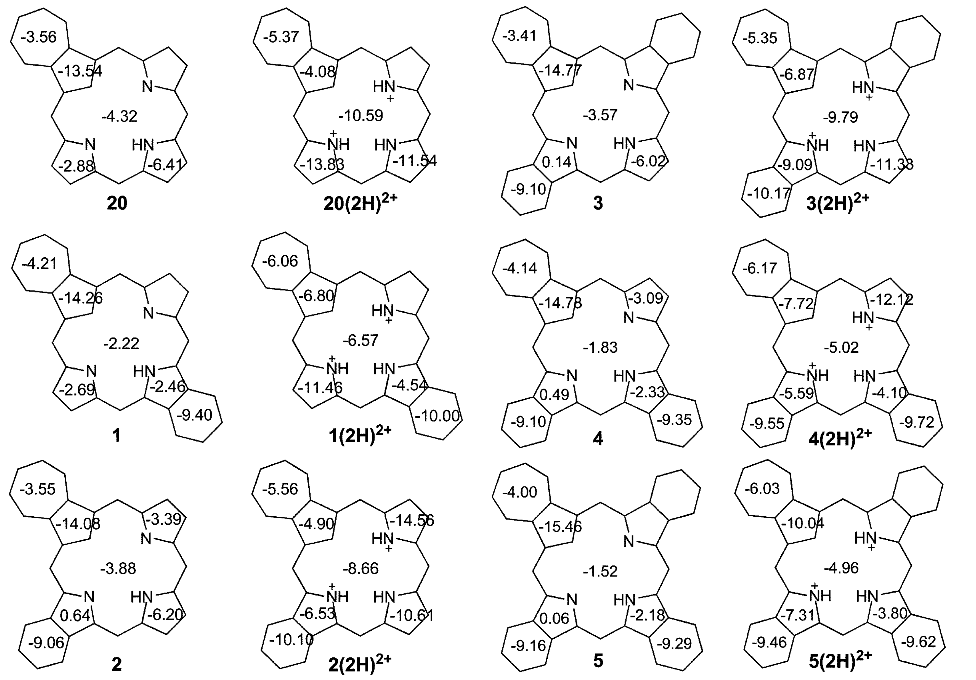

Figure 11. NICS values calculated at the HF/6-31+G(d) level of theory for azuliporphyrins and their diprotonated dications.

analysis calcd (%) for $C_{30}H_{35}NO_2\cdot 1/2H_2O$: C 79.96, H 8.05, N 3.11; found: C 79.53, H 8.14, N 3.21.

Azulitripyrrane 12: Montmorillonite K-10 clay (1.00 g) was added to a solution of **7** (382 mg, 0.865 mmol) and **9** (292 mg, 0.944 mmol) in anhydrous CH_2Cl_2 (40 mL). The resulting mixture was stirred at RT for 13 h under an Ar atmosphere. After the insoluble material was removed by filtration, the filtrate was poured into sat. aqueous $NaHCO_3$. The organic layer was washed successively with water and brine, dried over Na_2SO_4, and concentrated under reduced pressure. The residue was purified by column chromatography on silica gel with 20% hexane/$CHCl_3$. The product was obtained as a blue fraction. Recrystallization from $CHCl_3$/hexane gave **12** (316 mg, 53%). Blue crystals; m.p. 129.0–130.7 °C; ^{1}H NMR (400 MHz, $CDCl_3$): δ = 8.23 (brs, 1H; NH), 8.12 (dd, J = 11.0, 11.0 Hz, 2H; H-4,8), 8.00 (brs, 1H; NH), 7.39 (s, 1H; H-2), 7.22 (d, J = 10.7 Hz, 2H; H-5,7), 6.50–6.38 (m, 2H; olefin), 4.30 (s, 2H; CH_2), 4.27 (s, 2H; CH_2), 4.25 (m, 1H; bridgehead), 3.62 (m, 1H; bridgehead), 2.45 (t, J = 6.8 Hz, 2H; nBu^1), 2.24 (s, 3H; Me), 1.50 (s, 9H; CO_2tBu), 1.47 (s, 9H; CO_2tBu), 1.42 (s, 9H; 6-tBu), 1.60–1.25 (m, 8H; nBu and bridge), 0.91 ppm (t, J = 7.0 Hz, 3H; nBu); ^{13}C NMR (100 MHz, $CDCl_3$): δ = 164.06, 161.52, 156.90, 153.71,149.36, 147.60, 147.12, 144.84, 142.51, 142.47, 141.79, 140.10, 139.86, 139.13, 134.80, 134.77, 134.05, 133.81, 126.84, 126.23, 126.02, 125.97, 119.97, 119.62, 108.38, 105.04, 93.56, 91.06, 38.72, 34.85, 31.61, 25.76, 22.95, 18.84, 18.82, 17.05, 17.03, 14.25, 11.07 ppm; UV/Vis (CH_2Cl_2): λ_{max} [log (ε/M^{-1}cm^{-1})] = 290 (4.83), 299 (4.87), 340 (3.74), 355 (3.81), 373 (3.40), 600 nm (2.57); MS (FAB): m/z: 690 [M+H]$^+$; elemental analysis calcd (%) for $C_{45}H_{38}N_2O_4$: C 78.22, H 8.46, N 4.05; found: C 77.96, H 8.29, N 4.05.

Azuliporphyrin 15: Azulitripyrrane **10** (436 mg, 0.639 mmol) was stirred with TFA (1.5 mL) at RT for 10 min under an Ar atmosphere in the dark. After dilution with anhydrous CH_2Cl_2 (75 mL), **13** (131 mg, 0.652 mmol) was added to the mixture, which was stirred at the same temperature for 17 h. The reaction mixture was diluted with $CHCl_3$ (100 mL) and shaken with 0.1% aqueous ferric chloride solution (200 mL) for 10 min. The organic layer was separated, washed successively with sat. aqueous $NaHCO_3$, water and brine, dried over Na_2SO_4, and concentrated under reduced pressure. The residue was purified by column chromatography on alumina with 10% EtOAc/$CHCl_3$, followed by recrystallization from $CHCl_3$/hexane to give **10** (130 mg, 32%). Dark-green crystals; m.p. 200 °C (decomp); ^{1}H NMR (400 MHz, $CDCl_3$): δ = 9.31 (d, J = 10.5 Hz, 2H; H-2′,3′), 9.06 (s, 2H; H-5,20), 8.28 (s, 2H; H-10,15), 7.90 (d, J = 10.5 Hz, 2H; H-2“,3”), 6.90 (m, 2H; H-12“,13”), 5.09 (brs, 2H; H-12′,13′), 3.46 (t, J = 7.3 Hz, 4H; nBu), 2.95 (s, 6H; Me), 2.47 (brs, 1H; H-21), 2.26 (brs, 1H; NH), 2.01 (m, 4H; nBu), 1.96 (m, 2H; H-12“′,13”′), 1.66 (m, 6H; nBu and H-12′“,13′”), 1.59 (s, 9H; tBu), 1.06 ppm (t, J = 7.3 Hz, 6H; nBu); ^{13}C NMR (100 MHz, $CDCl_3$): δ = 164.16, 161.49, 154.00, 148.11, 146.06, 144.86, 137.53, 135.78 (C12“,13”), 135.04, 134.86, 134.05 (C2′,3′), 130.30 (C2“,3”), 126.11, 107.51 (C5,20), 93.36 (C10,15), 38.85 (tBu), 35.27 (C12′,13′), 34.95 (nBu^2), 31.73 (tBu), 27.36 (C12“′,13”′), 25.91 (nBu^1), 23.07 (nBu^3), 14.34 (nBu^4), 11.17 ppm (Me); UV/Vis (CH_2Cl_2): λ_{max} [log (ε/M^{-1}cm^{-1})] = 362 (4.82), 394 sh (4.69), 450 (4.74), 475 (4.84), 634 (4.23), 667 nm (4.24); UV/Vis (1% TFA/CH_2Cl_2): λ_{max} [log (ε/M^{-1}cm^{-1})] = 367 (4.90), 438 sh (4.77), 463 (5.10), 637 (4.51), 673 (4.19), 735 nm (3.87); MS (FAB): m/z: 646 [M+H]$^+$, 619 [M+H-C_2H_4]$^+$; elemental analysis calcd (%) for $C_{46}H_{51}N_3$: C 85.54, H 7.96, N 6.51; found: C 85.44, H 8.14, N 6.49.

Azuliporphyrin 18: Azulitripyrrane **12** (515 mg, 0.745 mmol) was stirred with TFA (1.5 mL) at RT for 10 min under an Ar atmosphere in the dark. After dilution with anhydrous CH_2Cl_2 (65 mL), **14** (158 mg, 0.879 mmol) was added to the mixture, which was stirred at the same temperature for 21 h. The reaction mixture was diluted with $CHCl_3$ (100 mL) and shaken with 0.1% aqueous ferric chloride solution (200 mL) for 5 min. The organic layer was separated, washed successively with sat. aqueous $NaHCO_3$, water, and ine, dried over Na_2SO_4, and concentrated under reduced pressure. The residue was purified by column chromatography on alumina with $CHCl_3$, followed by recrystallization from $CHCl_3$/hexane to give **18** (174 mg, 37%). Dark-green crystals; m.p. 180 °C (decomp); ^{1}H NMR (400 MHz, $CDCl_3$): δ = 9.32 (d, J = 10.5 Hz, 1H; H-2′ or H-3′), 9.27 (d, J = 10.2 Hz, 1H; H-2′ or H-3′), 9.13 (s, 1H; H-5), 9.02 (s, 1H; H-20), 8.22 (s, 1H; H-10), 8.19 (s, 1H; H-15), 7.86 (m, 2H; H-2“3”), 6.85 (m, 2H; H-7“8”), 5.06 (m, 1H; H-7′), 4.95 (m, 1H; H-8′), 3.56–3.46 (m, 4H; Et), 3.46–3.38 (m, 2H; nBu^1), 2.93 (s, 3H; Me), 2.66 (brs, 1H; H-21), 2.59 (brs, 1H; NH), 2.00 (m, 2H; nBu^2), 1.91 (m, 2H; H-7“), 1.72 (m, 2H; H-8”), 1.65 (m, 8H; bridge and nBu^3), 1.55 (s, 9H; tBu), 1.06 ppm (t, J = 7.3 Hz, 3H; nBu^4); ^{13}C NMR (100 MHz, $CDCl_3$): δ = 164.11, 161.59, 155.40, 154.06, 153.94, 149.01, 148.56, 148.09, 148.08, 144.76, 142.02, 141.89, 139.51, 139.33, 136.24, 135.71, 135.70, 135.01, 134.06, 133.99, 130.33, 130.17, 126.07, 126.03, 108.14, 107.47, 93.19, 92.86, 38.72, 36.33, 35.83, 34.85, 31.60, 27.42, 27.25, 25.82, 23.02, 18.85, 18.83, 17.08, 17.03, 14.25, 11.11 ppm; UV/Vis (CH_2Cl_2): λ_{max} [log (ε/M^{-1}cm^{-1})] = 361 (4.81), 383 sh (4.72), 451 (4.76), 473 (4.83), 629 (4.22), 668 nm (4.18); UV/Vis (1% TFA/CH_2Cl_2): λ_{max} [log (ε/M^{-1}cm^{-1})] = 366 (4.92), 436 sh (4.75), 463 (5.10), 584 (3.90), 633 (4.51), 674 (4.15), 736 nm (3.83); MS (FAB): m/z: 632 [M+H]$^+$, 604 [M+H-C_2H_4]$^+$; elemental analysis calcd (%) for $C_{45}H_{49}N_3\cdot 1/2H_2O$: C 84.33, H 7.86, N 6.56; found: C 84.05, H 7.85, N 6.19.

Azuliporphyrin 16: Azulitripyrrane **11** (304 mg, 0.435 mmol) was stirred with TFA (1 mL) at RT for 10 min under an Ar atmosphere in the dark. After dilution with anhydrous CH_2Cl_2 (50 mL), **14** (82 mg, 0.45 mmol) was added to the mixture, which was stirred at the same temperature for 19 h. The reaction mixture was diluted with $CHCl_3$ (150 mL) and shaken with 0.1 % aqueous ferric chloride solution (200 mL) for 10 min. The organic layer was separated, washed successively with sat. aqueous $NaHCO_3$, water and brine, dried over Na_2SO_4, and concentrated under reduced pressure. The residue was purified by column chromatography on alumina with $CHCl_3$, followed by recrystallization from $CHCl_3$/hexane to give **16** (129 mg, 46 %). Dark-green crystals; m.p. 200 °C (decomp); ^{1}H NMR (400 MHz, $CDCl_3$): δ = 9.39 (d, J = 10.0 Hz, 2H; H-2′3′), 9.18 (m, 2H; H-5,20), 8.28 (s, 2H; H-10,15), 7.91 (d, J = 10.0 Hz, 2H; H-2"3"), 6.86 (m, 4H; olefin), 5.09 (m, 2H; H-7′18′), 4.97 (m, 2H; H-8′17′), 3.54 (q, J = 7.6 Hz, 4H; Et), 2.45 (s, 1H; H-21), 1.90–1.73 (m, 8H; bridge), 1.67 (t, J = 7.6 Hz, 6H; Et), 1.60 ppm (s, 9H; *t*Bu); ^{13}C NMR (100 MHz, $CDCl_3$): δ = 153.94, 149.07, 148.61, 148.56, 136.34, 135.84, 134.42, 134.40, 126.17, 107.98, 107.94, 107.91, 93.24, 38.77, 36.35, 36.32, 35.85, 31.55, 27.44, 27.41, 27.26, 27.24, 18.87, 17.07 ppm; UV/Vis (CH_2Cl_2): λ_{max} [log (ε/$M^{-1}cm^{-1}$)] = 362 (4.83), 383 sh (4.77), 450 (4.76), 473 (4.87), 626 (4.23), 660 nm (4.23); UV/Vis (1 % TFA/CH_2Cl_2): λ_{max} [log (ε/$M^{-1}cm^{-1}$)] = 367 (4.93), 437 sh (4.77), 464 (5.13), 577 (3.94), 628 (4.51), 677 (4.08), 738 nm (3.87); MS (FAB): m/z: 640 [M+H]$^+$, 584 [M+H-2C_2H_4]$^+$; elemental analysis calcd (%) for $C_{46}H_{45}N_3$·1/2H_2O: C 85.15, H 7.15, N 6.48; found: C 84.96, H 7.00, N 6.40.

Azuliporphyrin 19: Azulitripyrrane **12** (150 mg, 0.217 mmol) was stirred with TFA (0.5 mL) at RT for 10 min under a N_2 atmosphere in the dark. After dilution with anhydrous CH_2Cl_2 (20 mL), **13** (49 mg, 0.24 mmol) was added to the mixture, which was stirred at the same temperature for 15 h. The reaction mixture was diluted with $CHCl_3$ (30 mL) and shaken with 0.1 % aqueous ferric chloride solution (50 mL) for 10 min. The organic layer was separated, washed successively with sat. aqueous $NaHCO_3$, water, and brine, dried over Na_2SO_4, and concentrated under reduced pressure. The residue was purified by column chromatography on alumina with 10 % hexane/$CHCl_3$, followed by recrystallization from $CHCl_3$/hexane to give **19** (43 mg, 30 %). Dark-green crystals; m.p. 180 °C (decomp); ^{1}H NMR (400 MHz, $CDCl_3$): δ = 9.30 (m, 2H; H-2′ or H-3′), 9.20 (m, 1H; H-5 or H-20), 9.08 (m, 1H; H-5 or H-20), 8.40 (m, 1H; H-10 or H-15), 8.33 (m, 1H; H-10 or H-15), 7.92 (m, 2H; H-2"3"), 6.89 (m, 4H; H-7"8"12"13"), 5.00 (m, 4H; H-7′8′12′13′), 3.46 (m, 2H; *n*Bu^1), 2.97 (s, 3H; Me), 2.22 (brs, 1H; NH), 2.03–1.59 (m, 12H; Bu^{2,3} and bridgehead), 1.59 (s, 9H; *t*Bu), 1.06 ppm (t, J = 7.3 Hz, 3H; *n*Bu^4); ^{13}C NMR (100 MHz, $CDCl_3$): δ = 153.99, 148.42, 144.78, 136.21, 136.18, 135.77, 135.73, 135.69, 135.05, 135.01, 134.24, 134.13, 130.69, 130.56, 130.54, 125.94, 107.88, 107.83, 93.66, 93.32, 38.79, 36.33, 35.88, 35.23, 35.20, 34.87, 31.63, 27.41, 27.26, 25.83, 23.00, 14.26, 11.13 ppm; UV/Vis (CH_2Cl_2): λ_{max} [log (ε/$M^{-1}cm^{-1}$)] = 363 (4.81), 389 (4.70), 448 (4.70), 474 (4.84), 626 (4.10), 666 nm (4.12); UV/Vis (1 % TFA/CH_2Cl_2): λ_{max} [log (ε/$M^{-1}cm^{-1}$)] = 335 (4.40), 367 (4.90), 438 (4.77), 463 (5.08), 585 (3.90), 634 (4.49), 680 (4.10), 739 nm (3.81); MS (FAB): m/z: 655 [M+H]$^+$, 599 [M+H-2C_2H_4]$^+$; elemental analysis calcd (%) for: $C_{47}H_{47}N_3$·1/2H_2O: C 85.16, H 7.30, N 6.34; found: C 84.88, H 7.41, N 6.21.

Azuliporphyrin 17: Azulitripyrrane **11** (1.05 g, 1.50 mmol) was stirred with TFA (3.5 mL) at RT for 10 min under an Ar atmosphere in the dark. After dilution with anhydrous CH_2Cl_2 (50 mL), **13** (369 mg, 1.83 mmol) was added to the mixture, which was stirred at the same temperature for 19 h. The reaction mixture was diluted with $CHCl_3$ (400 mL) and shaken with 0.1 % aqueous ferric chloride solution (400 mL) for 20 min. The organic layer was separated, washed successively with sat. aqueous $NaHCO_3$, water, and brine, dried over Na_2SO_4, and concentrated under reduced pressure. The residue was purified by column chromatography on alumina with $CHCl_3$ and 10 % EtOAc/hexane, followed by recrystallization from $CHCl_3$/hexane to give **17** (349 mg, 35 %). Dark-green crystals; m.p. 200 °C (decomp); ^{1}H NMR (400 MHz, $CDCl_3$): δ = 9.39 (d, J = 10.5 Hz, 2H; H-2′3′), 9.22 (s, 2H; H-5,20), 8.43 (s, 2H; H-10,15), 7.91 (d, J = 10.7 Hz, 2H; H-2"3"), 6.87–6.91 (m, 6H; olefin), 5.02–5.29 (m, 6H; bridgehead), 2.12 (brs, 1H; H-21), 1.33–1.99 (m, 12H; bridge), 1.62 ppm (s, 9H; *t*-Bu); ^{13}C NMR (100 MHz, $CDCl_3$): δ = 164.51, 155.12, 154.18, 154.17, 154.13, 149.26, 149.24, 148.92, 148.89, 148.67, 148.65, 146.22, 137.36, 136.33, 136.31, 135.89, 135.88, 135.82, 135.80, 135.54, 135.52, 134.40, 130.93, 126.08, 126.07, 107.86, 107.85, 93.79, 53.43, 38.86, 36.49, 36.03, 35.36, 31.70, 31.64, 27.54, 27.38, 22.72, 14.20 ppm; UV/Vis (CH_2Cl_2): λ_{max} [log (ε/$M^{-1}cm^{-1}$)] = 365 (4.80), 379 (4.74), 454 (4.73), 474 (4.82), 629 (4.20), 661 nm (4.20); UV/Vis (1 % TFA/CH_2Cl_2): λ_{max} [log (ε/$M^{-1}cm^{-1}$)] = 305 (4.18), 314 (4.16), 367 (4.93), 438 (4.79), 465 (5.14), 578 (3.93), 629 (4.51), 681 (4.07), 740 nm (3.89); MS (FAB): m/z: 662 [M+H]$^+$, 578 [M+H-3C_2H_4]$^+$; elemental analysis calcd (%) for $C_{48}H_{43}N_3$·$CHCl_3$·H_2O: C 76.95, H 6.19, N 5.49; found: C 76.88, H 6.28, N 5.30.

Retro-Diels–Alder reaction of BCOD-fused azuliporphyrins 15–19: BCOD-azuliporphyrins **15–19** (ca. 20 mg each) were heated at 200 °C under reduced pressure for 3 h in a glass tube to give azulibenzoporphyrins **1–5** in quantitative yields.

***Opp*-azulibenzoporphyrin 1**: Dark-green crystals; m.p. 206.3–208.3 °C; ^{1}H NMR (400 MHz, $CDCl_3$): δ = 9.16 (d, J = 10.4 Hz, 2H; H-2′3′), 8.73 (s, 2H; H-5,20), 8.70 (m, 2H; H-2"3"), 8.22 (s, 2H; H-10,15), 7.93–7.83 (m, 4H; benzo), 4.08 (brs, 1H; NH), 3.74 (s, 1H; H-21), 3.29 (m, 4H; *n*Bu^1), 2.82 (s, 6H; Me), 1.93 (m, 4H; *n*Bu^2), 1.67–1.57 (m, 4H; *n*Bu^3), 1.60 (s, 9H; *t*Bu), 1.05 ppm (t, J = 7.1 Hz, 6H; *n*Bu^4); ^{1}H NMR (400 MHz, 5 % TFA/$CDCl_3$): δ = 10.24 (s, 2H; H-5,20), 9.86 (d, J = 10.7 Hz, 2H; H-2′3′), 9.74 (s, 2H; H-10,15), 9.31 (m, 2H; benzo), 8.81 (d, J = 10.9 Hz, 2H; H-2"3"), 8.36 (m, 2H; benzo), 3.84 (t, J = 7.8 Hz, 4H; *n*Bu^1), 3.32 (s, 6H; Me), 2.04 (m, 4H; *n*Bu^2), 1.71 (s, 9H; *t*Bu), 1.73–1.62 (m, 4H; *n*Bu^3), 1.08 (t, J = 7.3 Hz, 6H; *n*Bu^4), 0.75 (brs, 1H; NH), −2.18 ppm (s, 1H; H-21); ^{13}C NMR (100 MHz, $CDCl_3$): δ = 163.95, 162.34, 153.54, 146.81, 144.98, 139.84, 136.64, 136.63, 135.40, 134.33, 133.72, 129.32, 128.03, 126.17, 120.97, 108.78, 91.10, 38.76, 34.75, 31.66, 25.69, 22.99, 14.23, 10.99 ppm; UV/Vis (CH_2Cl_2): λ_{max} [log (ε/$M^{-1}cm^{-1}$)] = 368 (4.68), 409 (4.70), 438 (4.76), 474 (4.71), 523 (4.09), 556 (4.09), 642 nm (4.21); UV/Vis (1 % TFA/CH_2Cl_2): λ_{max} [log (ε/$M^{-1}cm^{-1}$)] = 326 (4.44), 365 (4.78), 437 (4.71), 468 (5.05), 506 (4.52), 585 (3.89), 640 (4.35), 671 nm (4.47); MS (FAB): m/z: 618 [M+H]$^+$; elemental analysis calcd (%) for $C_{44}H_{47}N_3$·1/4$CHCl_3$: C 82.05, H 7.35, N 6.49; found: C 81.83, H 7.27, N 6.44.

***Adj*-azulibenzoporphyrin 2**: Dark-green crystals; m.p. >300 °C; ^{1}H NMR (400 MHz, $CDCl_3$): δ = 9.31 (s, 1H; H-5). 9.26 (d, J = 10.5 Hz, 1H; H-3′). 9.22 (d, J = 10.5 Hz, 1H; H-2′), 8.99 (s, 1H; H-20), 8.69 (m, 1H; H-7′), 8.62 (m, 1H; H-8′), 8.48 (s, 1H; H-10), 8.16 (s, 1H; H-15), 7.90–7.66 (m, 4H; H-2",3",7",8"), 3.52 (q, J = 7.5 Hz, 2H; Et), 3.48 (q, J = 7.5 Hz, 2H; Et), 3.42 (t, J = 7.6 Hz, 2H; *n*Bu), 2.91 (s, 3H; Me), 2.81 (s, 1H; H-21), 1.99 (m, 2H; *n*Bu), 1.72–1.58 (m, 8H; Et and *n*Bu), 1.56 (s, 9H; *t*Bu), 1.39 (brs, 1H; NH), 1.05 ppm (t, J = 7.3 Hz, 3H; *n*Bu); ^{13}C NMR (100 MHz, $CDCl_3$): δ = 164.07, 161.52, 156.90, 153.71, 149.36, 147.60, 147.12, 144.84, 142.51, 142.47, 141.79, 140.10, 139.86, 139.13, 134.80, 134.77, 134.05, 133.81, 129.81, 126.84, 126.23, 126.02, 125.98, 119.97, 119.62, 108.38, 105.04, 93.56, 91.06, 38.72, 34.85, 31.61, 25.76, 22.95, 18.84, 18.82, 17.05, 17.02, 14.25, 11.07 ppm; ^{1}H NMR (400 MHz, 5 % TFA/$CDCl_3$): δ = 10.57 (s, 1H; H-5), 10.41 (s, 1H; H-20), 9.98 (d, J = 10.7 Hz, 1H; H-2′), 9.92 (d, J = 10.8 Hz, 1H; H-3′), 9.87 (s, 1H; H-10), 9.63 (s, 1H; H-15), 9.36 (m, 1H; H-7′), 9.31 (m, 1H; H-8′), 8.83 (m, 2H; H-2",3"), 8.43 (m, 1H; H-7"), 8.35 (m, 1H; H-8"), 3.90 (m, 6H; Et and *n*Bu), 3.36 (s, 3H; Me), 2.02 (m, 2H; *n*Bu), 1.76 (m, 6H; Et), 1.72 (s, 9H; *t*Bu), 1.67 (m, 2H; *n*Bu), 1.05 (t, J = 7.4 Hz, 3H; *n*Bu), 0.43 (brs, 1H; NH), −0.19 (s, 1H; NH), −1.64 (brs, 1H; NH), −2.87 ppm (s, 1H; H-21); UV/Vis (CH_2Cl_2): λ_{max} [log (ε/$M^{-1}cm^{-1}$)] = 306 (4.41), 351 sh (4.70), 372 (4.85), 420 (4.68), 445 (4.79), 467 (4.80), 653 (4.46), 692 (4.55), 758 nm (3.94); UV/Vis (1 % TFA/CH_2Cl_2): λ_{max} [log (ε/$M^{-1}cm^{-1}$)] = 313 (4.33), 376 (4.97), 427 sh (4.74), 463 (4.94), 500 sh (4.54), 662 (4.46), 694 nm (4.63); MS (FAB): m/z: 605 [M+H]$^+$; elemental analysis calcd (%) for $C_{43}H_{45}N_3$: C 85.53, H 7.51, N 6.96; found: C 85.39, H 7.58, N 6.74.

***Adj*-azulidibenzoporphyrin 3**: Dark-green crystals; m.p. >300 °C; ^{1}H NMR (400 MHz, $CDCl_3$): δ = 9.09 (s, 2H; H-5,20), 9.07 (d, J = 11.0 Hz, 2H; H-2′,3′), 8.60 (d, J = 7.0 Hz, 2H; H-7′,18′), 8.55 (d, J = 7.3 Hz, 2H; H-8′,17′), 8.35 (s, 2H; H-10,15), 7.91 (d, J = 11.0 Hz, 2H; H-2",3"), 7.75 (m, 4H; H-7",8",17",18"), 3.45 (q, J = 7.5 Hz, 4H; Et), 2.50 (s, 1H; H-21), 2.40 (brs, 1H; NH), 1.66 (t, J = 7.5 Hz, 6H; Et), 1.57 ppm (s, 9H; *t*Bu); ^{13}C NMR (100 MHz, $CDCl_3$): δ = 164.05, 156.65, 149.03, 146.95, 142.38, 142.23, 139.95, 139.60, 134.18, 133.90, 129.64, 126.89, 126.04, 125.98, 120.00, 119.64, 105.53, 91.75, 38.80, 31.73, 30.97, 18.91, 17.13 ppm; ^{1}H NMR (400 MHz, 5 % TFA/$CDCl_3$): δ = 10.66 (s, 2H; H-5,20), 9.96 (s, 2H; H-10,15), 9.96 (d, J = 11.0 Hz, 2H; H-2′,3′), 9.37 (d, J = 7.9 Hz, 2H; H-7′,18′), 9.32 (d, J = 8.1 Hz, 2H; H-8′,17′), 8.79 (d, J =

10.7 Hz, 2H; H-2“,3”), 8.43 (m, 4H; H-7“,8”,17“,18”), 3.93 (q, $J=7.6$ Hz, 4H; Et), 1.78 (t, $J=7.6$ Hz, 6H; Et), 1.74 (s, 9H; *t*Bu), 0.71 (brs, 1H; NH), −2.31 (s, 1H; H-21); UV/Vis (CH_2Cl_2): λ_{max} [log (ε/$M^{-1}cm^{-1}$)] = 359 (4.65), 380 (4.84), 399 (4.95), 446 (4.75), 474 (4.83), 595 (4.04), 694 nm (4.26); UV/Vis (1% TFA/CH_2Cl_2): λ_{max} [log (ε/$M^{-1}cm^{-1}$)] = 306 sh (4.39), 386 sh (4.92), 436 (4.88), 473 sh (4.70), 502 (4.63), 671 (4.17), 731 nm (4.87); MS (FAB): *m*/*z*: 584 [*M*+H]$^+$; elemental analysis calcd (%) for $C_{42}H_{37}N_3\cdot 1/4H_2O$: C 85.75, H 6.43, N, 7.14; found: C 85.80, H 6.38, N 7.07.

***Adj*,*opp*-azulidibenzoporphyrin 4**: Dark-green crystals; m.p. >300°C; ^{1}H NMR (400 MHz, $CDCl_3$): $\delta=8.94$ (m, 2H), 8.70–7.50 (m, 14H), 3.05 (m, 2H), 2.55 (m, 3H), 1.80 (m, 2H), 1.72–1.50 (m, 13H), 1.04 ppm (m, 3H); UV/Vis (CH_2Cl_2): λ_{max} [log (ε/$M^{-1}cm^{-1}$)] = 351 sh (4.51), 370 sh (4.63), 390 (4.67), 421 (4.68), 441 (4.71), 473 (4.65), 498 sh (4.25), 580 (4.13), 617 nm (4.09); UV/Vis (1% TFA/CH_2Cl_2): λ_{max} [log (ε/$M^{-1}cm^{-1}$)] = 326 (4.40), 350 (4.47), 377 (4.64), 446 (4.75), 463 (4.79), 515 (4.29), 585 (3.86), 654 (4.25), 699 (4.55), 768 nm (3.47); MS (FAB): *m*/*z*: 598 [*M*+H]$^+$; elemental analysis calcd (%) for $C_{43}H_{39}N_3\cdot H_2O$: C 83.87, H 6.71, N 6.82; found: C 83.52, H 6.61, N 6.66.

Azulitribenzoporphyrin 5: Dark-green crystals; m.p. >300°C; ^{1}H NMR (400 MHz, $CDCl_3$): $\delta=9.30$–9.05 (m, 4H), 8.81 (m, 2H), 8.70–8.50 (m, 6H), 8.05–7.70 (m, 8H), 1.64 ppm (s, 9H); UV/Vis (CH_2Cl_2): λ_{max} [log (ε/$M^{-1}cm^{-1}$)] = 394 sh (4.68), 422 sh (4.54), 445 (4.58), 474 (4.58), 507 (4.20), 668 (4.11), 713 nm (4.08); UV/Vis (1% TFA/CH_2Cl_2): λ_{max} [log (ε/$M^{-1}cm^{-1}$)] = 379 (4.77), 390 (4.77), 442 (4.85), 456 (4.84), 520 (4.60), 674 (4.22), 736 nm (5.01); MS (FAB): *m*/*z*: 578 [*M*+H]$^+$; elemental analysis calcd (%) for $C_{42}H_{31}N_3$: C 87.32, H 5.41, N 7.27; found: C 87.24, H 5.49, N 7.26.

Acknowledgements

We thank the Venture Business Laboratory, Ehime University, for their assistance in obtaining MALDI-TOF mass spectra. We appreciate the generosity of Nippon Synthetic Chem. Ind. (Osaka Japan) for supplying us with ethyl isocyanoacetate, which was used in the preparation of the starting pyrroles. This work was partially supported by Grants-in-Aid for the Scientific Research on Innovative Areas (No. 21108517, π-Space to H.U.) from MEXT and a C-tier grant (No. 20550047 to H.U.) from JSPS.

[1] a) T. D. Lash in *The Porphyrin Handbook, Vol. 2* (Eds: K. M. Kadish, K. M. Smith, R. Guilard), Academic Press, San Diego, **2000**, pp. 165–193; b) M. Pawlicki, L. Latos-Grażyński in *Handbook of Porphyrin Science* (Eds.: K. M. Kadish, K. M. Smith, R. Guilard), World Scientific, Singapore, **2010**, pp. 103–192.

[2] a) T. D. Lash, S. T. Chaney, *Angew. Chem.* **1997**, *109*, 867–868; *Angew. Chem. Int. Ed. Engl.* **1997**, *36*, 839–840; b) S. R. Graham, D. A. Colby, T. D. Lash, *Angew. Chem.* **2002**, *114*, 1429–1432; *Angew. Chem. Int. Ed.* **2002**, *41*, 1371–1374; c) T. D. Lash, J. A. El-Beck, G. M. Ferrence, *J. Org. Chem.* **2007**, *72*, 8402–8415.

[3] a) D. A. Colby, T. D. Lash, *Chem. Eur. J.* **2002**, *8*, 5397–5402; b) T. D. Lash, D. A. Colby, S. R. Graham, S. T. Chasey, *J. Org. Chem.* **2004**, *69*, 8851–8864; c) T. D. Lash, D. A. Colby, S. R. Graham, G. M. Ferrence, L. F. Szczepura, *Inorg. Chem.* **2003**, *42*, 7326–7338; d) G. M. Ferrence, T. D. Lash, *Acta Crystallogr., Sect. E: Struct. Rep. Online* **2007**, *63*, m1351–m1353; e) Z. Zhang, G. M. Ferrence, T. D. Lash, *Org. Lett.* **2009**, *11*, 101–104; f) D. T. Richter, T. D. Lash, *J. Org. Chem.* **2004**, *69*, 8842–8850.

[4] S. Venkatraman, V. G. Anand, V. PrabhuRaja, H. Rath, J. Sankar, T. K. Chandrashekar, W. Teng, K. R. Senge, *Chem. Commun.* **2002**, 1660–1661.

[5] a) A. Berlicka, N. Sprutta, L. Latos-Grażyński, *Chem. Commun.* **2006**, 3346–3348; b) N. Sprutta, M. Świderska, L. Latos-Grażyński, *J. Am. Chem. Soc.* **2005**, *127*, 13108–13109; c) N. Sprutta, M. Siczek, L. Latos-Grażyński, M. Pawlicki, L. Sterengerg, T. Lis, *J. Org. Chem.* **2007**, *72*, 9501–9509; d) N. Sprutta, S. Maćkowiak, M. Kocik, L. Szterenberg, T. Lis, L. Latos-Grażyński, *Angew. Chem.* **2009**, *121*, 3387–3391; *Angew. Chem. Int. Ed.* **2009**, *48*, 3337–3341.

[6] K. Hafner, C. Bernhard, *Justus Liebigs Ann. Chem.* **1959**, *625*, 108–123.

[7] T. Okujima, N. Komobuchi, Y. Shimizu, H. Uno, N. Ono, *Tetrahedron Lett.* **2004**, *45*, 5461–5464.

[8] S. Ito, N. Morita, T. Asao, *Bull. Chem. Soc. Jpn.* **1995**, *68*, 2011–2016.

[9] A. Moudif, M. Momenteau, *J. Chem. Soc., Perkin Trans. 1* **1996**, 1235–1242.

[10] T. Okujima, N. Komobuchi, H. Uno, N. Ono, *Heterocycles* **2006**, *67*, 255–267.

[11] S. Ito, N. Ochi, T. Murashima, H. Uno, N. Ono, *Heterocycles* **2000**, *52*, 399–411.

[12] T. Okujima, Y. Hashimoto, G. Jin, H. Yamada, N. Ono, *Heterocycles* **2009**, *77*, 1235–1248.

[13] The diffraction data were corrected for Lorentz, polarization, and absorption effects. The structures were solved with SIR2004[14] and refined with SHELXL-97.[15] All calculations were performed by using the Crystal Structure crystallographic software package.[16] CCDC-874980 (**1**), CCDC-874979 (**2**) and CCDC-874981 (**3**) contain the supplementary crystallographic data for this paper. These data can be obtained free of charge from The Cambridge Crystallographic Data Centre via www.ccdc.cam.ac.uk/data_request/cif.

[14] SIR2004: an improved tool for crystal structure determination and refinement, see: M. C. Burla, R. Caliandro, M. Camalli, B. Carrozzini, G. L. Cascarano, L. De Caro, C. Giacovazzo, G. Polidori, R. Spagna, *J. Appl. Crystallogr.* **2005**, *38*, 381–388.

[15] SHELXL-97: Program for solution and refinement of crystal structures from diffraction data, University of Göttingen, Göttingen, Germany; *"A short history of SHELX"*. G. M. Sheldrick, *Acta Crystallogr., Sect. A: Found. Crystallogr.* **2008**, *64*, 112–122.

[16] Rigaku (2010) Crystal Structure, version 3.8.2 or 4.0.1, Rigaku Corporation, Tokyo, Japan.

[17] A. W. Hanson, *Acta. Cryst.* **1965**, *19*, 19–26.

[18] a) P. von R. Schleyer, C. Maerker, A. Dransfeld, H. Jiao, N. J. R. van E. Hommes, *J. Am. Chem. Soc.* **1996**, *118*, 6317–6318; b) Z. Chen, C. S. Wannere, C. Corminboeuf, R. Puchta, P. von R. Schleyer, *Chem. Rev.* **2005**, *105*, 3842–3888.

[19] a) M. K. Cyrañski, T. M. Krygowski, M. Wisiorowski, N. J. R. van E. Hommes, P. von R. Schleyer, *Angew. Chem.* **1998**, *110*, 187–190; *Angew. Chem. Int. Ed.* **1998**, *37*, 177–180; b) J. Jusélius, D. Sundholm, *J. Org. Chem.* **2000**, *65*, 5233–5237.

[20] H. Furuta, H. Maeda, A. Osuka, *J. Org. Chem.* **2001**, *66*, 8563–8572.

[21] M. Stepien, L. Latos-Grazynski, L. Szterenberg, *J. Org. Chem.* **2007**, *72*, 2259–2270.

[22] a) Y. Matano, T. Nakabuchi, T. Miyajima, H. Imahori, H. Nakano, *Org. Lett.* **2006**, *8*, 5713–5716; b) Y. Matano, M. Nakashima, T. Nakabuchi, H. Imahori, S. Fujishige, H. Nakano, *Org. Lett.* **2008**, *10*, 553–556.

Received: April 24, 2012
Revised: June 19, 2012
Published online: August 22, 2012

